RSC Advances

ROYAL SOCIETY OF CHEMISTRY

www.rsc.org/advances

Understanding the high reactivity of carbonyl compounds towards nucleophilic carbenoid intermediates generated from carbene isocyanides

Mar Ríos-Gutiérrez,[a] Luis R. Domingo,[a*] and Patricia Pérez[b]

[a] Universidad de Valencia, Facultad de Química, Departamento de Química Orgánica, Dr. Moliner 50, E-46100 Burjassot, Valencia, Spain.
[b] Universidad Andrés Bello, Facultad de Ciencias Exactas, Departamento de Ciencias Químicas, Av. República 230, 8370146, Santiago, Chile.
e-mail: domingo@utopia.uv.es
web: www.luisrdomingo.com

Abstract

The high reactivity of carbonyl compounds towards carbenoid intermediate *cis*-**IN** generated *in situ* by the addition of methyl isocyanide to dimethyl acetylenedicarboxylate (DMAD) has been investigated at the MPWB1K/6-311G(d,p) computational level by using the Molecular Electron-Density Theory (MEDT). This multicomponent (MC) reaction is a domino process that comprises two sequential reactions: *i)* the formation of nucleophilic carbenoid intermediate *trans*-**IN**; and *ii)* the nucleophilic attack of *cis*-**IN** on the carbonyl compound resulting in the formation of the final 2-imino-furan derivative. The present MEDT study permits establishing that the high nucleophilic character and the electronic structure of carbenoid intermediate *cis*-**IN** together with the specific approach mode of the carbonyl C=O double bond along the nucleophilic attack of the sp^2 hybridised carbenoid C4 center of *cis*-**IN** on the carbonyl C5 carbon of acetone enables the formation of the C4−C5 single bond with a very low activation enthalpy, 3.3 kcal/mol, without any external electrophilic activation of the carbonyl group, and the subsequent ring closure through the downhill formation of the C−O single bond. The Bonding Evolution Theory (BET) study along the formation of the 2-imino-furan allows characterising the mechanism as a [2n+2n] cycloaddition, ruling out the proposed 1,3-dipolar cycloaddition mechanism.

Introduction

Carbene isocyanides **I** are essential building blocks in modern organic chemistry,[1] and it has been reported that these species nucleophilically attack dialkyl acetylenedicarboxylates **II** yielding zwitterionic species **III**, which act as crucial intermediates. These reactive intermediates are readily trapped by several kinds of electrophilic carbon molecules[2] such as aldehydes,[3] ketones,[4] esters,[5] and sulfonylimines,[6] even carbon dioxide.[7] When electrophilic molecules are carbonyl derivatives **IV**, the reaction products are 2-imino-furan derivatives **V** (see Scheme 1). Polyfunctionalised furans are versatile synthetic starting materials for the preparation of a great variety of heterocyclic and acyclic compounds,[8] and especially 2,5-disubstituted furan-3,4-dicarboxylates which are very important starting materials in the synthesis of natural products containing tetrahydrofuran rings.[9]

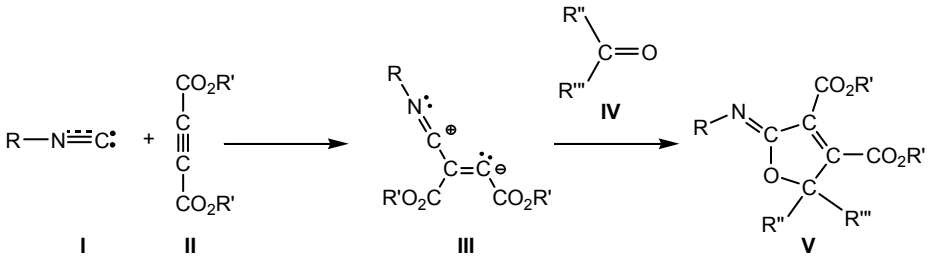

Scheme 1.

This multicomponent (MC) reaction is a domino process that comprises two consecutive reactions: *i)* a nucleophilic attack of carbene isocyanides **I** on acetylenedicarboxylates **II** yielding the proposed zwitterionic intermediates **III**; and *ii)* the quick capture of these intermediates by a carbonyl derivative **IV** yielding 2-imino-furan derivatives **V**. This last step has been associated with a 1,3-dipolar cycloaddition reaction in which zwitterionic intermediate **III** participates as the 1,3-dipole and the carbonyl derivative as the dipolarophile.[3,4]

For this 1,3-dipolar cycloaddition reaction two mechanisms have been proposed (see Scheme 2): *i)* a one-step mechanism in which the C−C and C−O bonds are formed in a single step but asynchronously;[4a] and *ii)* a stepwise mechanism in which a new zwitterionic intermediate **VI** is formed through the nucleophilic attack of isocyanide **I** on acetylenedicarboxylate **II**; the subsequent cyclisation in this intermediate will yield 2-imino-furan derivative **V**.[4b]

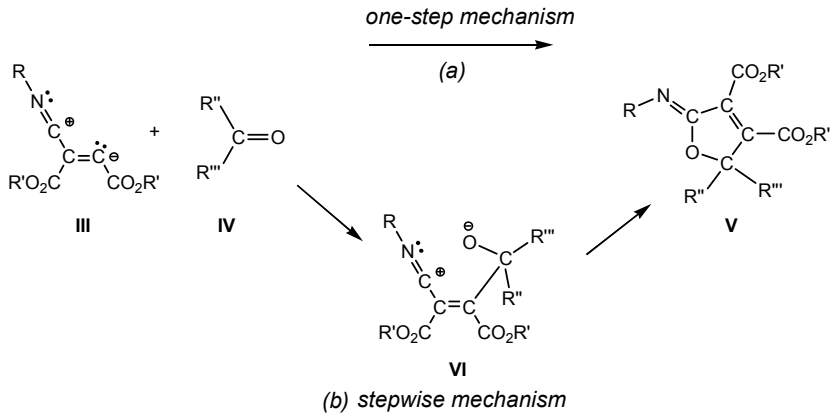

Scheme 2. Proposed mechanisms for the 1,3-dipolar cycloadditions of intermediate **III** with carbonyl derivatives **IV**.

Due to the high reactivity evidenced by intermediate **III** and the significance of the formation of 2-imino-furans **V** through these MC reactions involving a large diversity of carbonyl derivatives **IV**,[3-5,7] a Density Functional Theory (DFT) study of the MC reaction between methyl isocyanide **1**, DMAD **2** and acetone **3** yielding 2-imino-furan **4** is performed herein, using the Molecular Electron-Density Theory (MEDT) to explain this high reactivity (see Scheme 3). The proposed MEDT, in which the changes in the electron-density and not molecular orbital interactions are responsible for the reactivity in organic chemistry, uses quantum chemical tools based on the analysis of the electron-density such as the conceptual DFT reactivity indices[10] and the topological Electron Localisation Function[11] (ELF) analysis of the changes of the molecular electron-density along the reaction path in order to establish the molecular mechanism of an organic reaction.

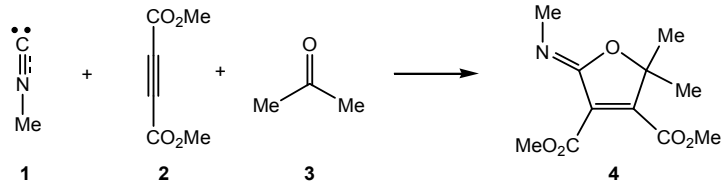

Scheme 3. Selected reaction model for the MC reaction of isocyanides **I**, acetylenedicarboxylate derivatives **II** and carbonyl compounds **IV**.

To this end, a theoretical study at the MPWB1K/6-311G(d,p) computational level, in which a combination of *i)* the exploration and characterisation of the potential energy surfaces (PESs) associated with the selected domino reaction, *ii)* the analysis of the reactivity indices derived from the conceptual DFT at the ground state of the reagents and *iii)* the Bonding Evolution Theory[12] (BET) analysis of the two consecutive

reactions was carried out. Three unresolved questions will be answered: *i)* what is the electronic structure of intermediate **III** formed in these domino reactions?; *ii)* what is the origin of the high reactivity of carbonyl compounds **IV** in these MC reactions?; and finally, *iii)* what is the mechanism of the cycloaddition step?. As these questions cannot be experimentally resolved, our theoretical study provides valuable information about these MC reactions.

Computational Methods

Several studies have shown that the B3LYP functional[13] is relatively accurate for providing kinetic data, although the reaction exothermicities are underestimated.[14] Truhlar's group has proposed some functionals, such as the MPWB1K one,[15] which gives good results for combinations of thermochemistry, thermochemical kinetics and other weak interactions. Therefore, in this study the MPWB1K functional was selected together with the standard 6-31G(d) basis set.[16] The optimisations were carried out using the Berny analytical gradient optimisation method.[17] The stationary points were characterised by frequency computations in order to verify that TSs have one and only one imaginary frequency. The IRC paths[18] were traced in order to check the energy profiles connecting each TS to the two associated minima of the proposed mechanism using the second order González-Schlegel integration method.[19] Solvent effects were taken into account by full optimisation of the gas phase structures at the MPWB1K/6-311G(d,p) level using the polarisable continuum model (PCM) developed by Tomasi's group[20] in the framework of the self-consistent reaction field (SCRF).[21] The integral equation formalism variant is the SCRF method used in this work. Several polar solvents as dichloromethane, benzene and acetonitrile have been used in these MC reactions. Acetonitrile was selected for the solvent effects calculations since that in the reactions of a benzo[b]acridine-6,11-dione acting as the carbonyl derivative it was used.[4b] Values of enthalpies, entropies and Gibbs free energies in acetonitrile were calculated with the standard statistical thermodynamics at 25 ºC and 1 atm.[16] No scaling factor in the thermodynamic calculations was used. The electronic structures of stationary points were characterised by the natural bond orbital (NBO) analysis.[22]

Conceptual DFT[23] provides different indices to rationalize and understand chemical structure and reactivity.[10] In this sense, the global electrophilicity index,[24] ω, is given by the following expression, $\omega = (\mu^2 / 2\eta)$, in terms of the electronic chemical

potential μ and the chemical hardness η. Both quantities may be approached in terms of the one-electron energies of the frontier molecular orbital HOMO and LUMO, ε_H and ε_L, as $\mu \approx (\varepsilon_H + \varepsilon_L)/2$ and $\eta \approx (\varepsilon_L - \varepsilon_H)$, respectively.[25] The empirical (relative) nucleophilicity index,[26] N, based on the HOMO energies obtained within the Kohn-Sham scheme,[27] is defined as $N = E_{HOMO}(Nu) - E_{HOMO}(TCE)$, where tetracyanoethylene (TCE) is the reference, because it presents the lowest HOMO energy in a long series of molecules already investigated in the context of polar organic reactions. This choice allows handling conveniently a nucleophilicity scale of positive values. Nucleophilic P_k^- and electrophilic P_k^+ Parr functions[28] were obtained through the analysis of the Mulliken atomic spin density of the corresponding radical cations or anions.

The characterisation of the electron-density reorganisation to evidence the bonding changes along a reaction path is the most attractive method to characterise a reaction mechanism.[29] To perform these analyses quantitatively, the BET,[12] consisting of the joint-use of ELF topology and Thom's catastrophe theory[30] (CT), proposed by Krokidis et al.,[12] is a new tool for analysing the electronic changes in chemical processes. BET has been applied to different elementary reactions,[31] allowing the molecular mechanism to be established. The ELF topological analysis, $\eta(\mathbf{r})$,[32] was performed with the TopMod program[33] using the corresponding MPWB1K/6-311G(d,p) monodeterminantal wavefunctions of the selected structures of the IRC. Non-covalent interactions (NCI) were computed using the methodology previously described.[34] All computations were carried out with the Gaussian 09 suite of programs.[35]

Results and discussion

The present theoretical study has been divided into four parts: *i)* first, the PESs associated with the domino reaction between isocyanide **1**, DMAD **2** and acetone **3** yielding 2-imino-furan **4** are explored and characterised; *ii)* then, an analysis of the DFT reactivity indices at the ground state of the reagents involved in this domino process is carried out; iii) next, a BET study of the two consecutive reactions is performed in order to characterise the molecular mechanism; and finally, *iv)* the electronic structure of intermediate *cis*-**IN** as well as the origin of the high reactivity of carbonyl compounds in these MC reactions are discussed.

*i) Study of the PESs of the MC reaction between methyl isocyanide **1**, DMAD **2** and acetone **3**.*

The MC reaction between methyl isocyanide **1**, DMAD **2** and acetone **3** to yield 2-imino-furan **4** is a domino reaction that comprises two addition reactions (see Scheme 4). The first one is the nucleophilic attack of carbene methyl isocyanide **1** on one of the two electrophilic acetylenic carbon atoms of DMAD **2** to yield intermediate *trans*-**IN,** which after isomerisation to intermediate *cis*-**IN** attacks acetone **3**. Total and relative electronic energies of the stationary points involved in the two consecutive processes of the MC reaction between isocyanide **1**, DMAD **2** and acetone **3** are given in Table 1.

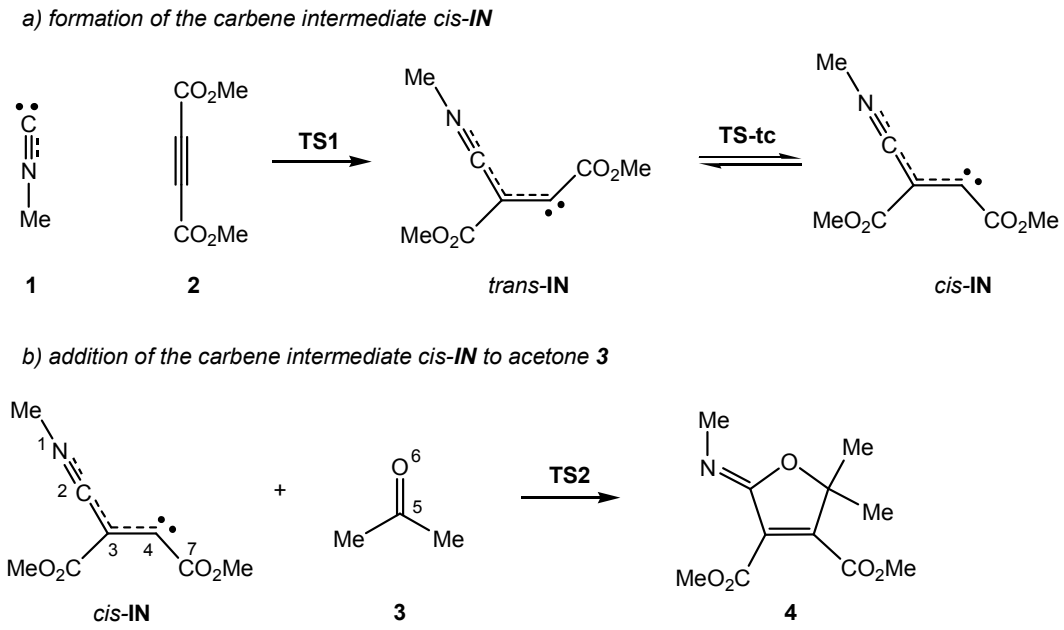

Scheme 4. Domino reaction between methyl isocyanide **1**, DMAD **2** and acetone **3**.

The activation energy associated with the nucleophilic attack of carbene methyl isocyanide **1** on DMAD **2**, *via* **TS1**, presents a high value, 17.4 kcal/mol, the formation of intermediate *trans*-**IN** being slightly exothermic, −0.4 kcal/mol. This intermediate, which presents a *trans* disposition of the two carboxylate groups, undergoes a sp^2-sp-sp^2 rehybridisation process at the C4 carbon *via* **TS-tc** with an estimated activation energy of 9.4 kcal/mol to yield *cis*-**IN**, which is 1.4 kcal/mol lower in energy than *trans*-**IN**. Noteworthy, the *cis* rearrangement of the two carboxylate groups at *cis*-**IN** is required for the subsequent addition of acetone **3** followed by the concomitant ring closure. From this intermediate, the formation of 2-imino-furan **4** takes place through the nucleophilic

attack of *cis*-**IN** on acetone **3**, followed by a downhill C−O bond formation. This nucleophilic attack *via* **TS2** presents a very low activation energy, 4.1 kcal/mol, the cycloaddition being strongly exothermic by 88.3 kcal/mol.

Activation and reaction energies associated with **TS1** and **TS2**, and 2-imino-furan **4**, decrease by 1 kcal/mol and 6 kcal/mol, respectively, when solvent effects of acetonitrile are considered. On the contrary, activation and reaction energies associated with **TS-tc**, and *trans*-**IN** and *cis*-**IN**, increase by between 5−7 kcal/mol. This behaviour is the consequence of a higher solvation of intermediates *trans*-**IN** and *cis*-**IN** than of the reagents, TSs, and the final product along this MC reaction.

Table 1. MPWB1K/6-311G(d,p) total (E, in au) and relative[a] electronic energies (ΔE, in kcal/mol), in gas phase and in acetonitrile, of the stationary points involved in the domino reaction between **1**, **2** and **3**.

	Gas phase		*Acetonitrile*	
	E	ΔE	E	ΔE
1	-132.674951		-132.681758	
2	-532.962501		-532.971986	
3	-193.098437		-193.104691	
TS1	-665.609778	17.4	-665.624629	18.3
trans-**IN**	-665.638068	-0.4	-665.664217	-6.6
TS-tc	-665.622520	9.4	-665.649492	2.7
cis-**IN**	-665.639621	-1.4	-665.666500	-6.6
TS2	-858.744588	-5.5	-858.765118	-4.2
4	-858.876561	-88.3	-858.888753	-81.8

[a] Relative to **1**, **2** and **3**.

Enthalpies, entropies, Gibbs free energies and the relative ones of the stationary points involved in the domino reaction between methyl isocyanide **1**, DMAD **2** and acetone **3** are displayed in Table 2. The Gibbs free energy profile including both consecutive processes is graphically represented in Figure 1. Inclusion of the thermal corrections to the electronic energies does not significantly change the relative enthalpies of the stationary points involved in this MC reaction, those of **TS1**, **TS-tc** and *cis*-**IN** remain almost unchanged but those of *trans*-**IN**, **TS2** and **4** slightly increase by between 1−5 kcal/mol. Inclusion of the entropies to the enthalpies increases the relative Gibbs free energies by between 11 and 33 kcal/mol, due to the unfavourable entropy associated with this bimolecular reaction.

Table 2. MPWB1K/6-311G(d,p) enthalpies (H, in au), entropies (S, in cal/mol·K) and Gibbs free energies (G, in au), and relative[a] enthalpies (ΔH, in kcal/mol), entropies (ΔS, in cal/mol·K) and Gibbs free energies (ΔG, in kcal/mol), at 25ºC and 1 atm in acetonitrile, of the stationary points involved in the domino reaction between **1**, **2** and **3**.

	H	ΔH	S	ΔS	G	ΔG
1	-132.630638		58.298		-132.658324	
2	-532.841793		104.873		-532.891597	
3	-193.013050		71.406		-193.046960	
TS1	-665.442939	18.5	127.102	-36.1	-665.503299	29.3
trans-**IN**	-665.481317	-5.6	120.401	-42.8	-665.538495	7.2
TS-tc	-665.467932	2.8	118.198	-45.0	-665.524063	16.2
cis-**IN**	-665.482621	-6.4	125.618	-37.6	-665.542277	4.8
TS2	-858.488597	-2.0	150.779	-83.8	-858.560201	23.0
4	-858.607120	-76.3	143.575	-91.0	-858.675303	-49.2

[a] Relative to **1**, **2** and **3**.

Thus, the activation Gibbs free energy associated with the first nucleophilic attack of isocyanide **1** on DMAD **2**, *via* **TS1**, is 29.3 kcal/mol, formation of intermediate *trans*-**IN** being endergonic by 7.2 kcal/mol. The following conversion of *trans*-**IN** into *cis*-**IN** presents an activation Gibbs free energy of 9.0 kcal/mol (**TS-tc**), the conversion being exergonic by 2.4 kcal/mol. Finally, the cycloaddition reaction of *cis*-**IN** with acetone **3** *via* **TS2** yields 2-imino-furan **4** with an activation Gibbs free energy of 23.0 kcal/mol. Formation of the final cycloadduct **4** is strongly exergonic by 49.2 kcal/mol.

Some interesting conclusions can be drawn from the Gibbs free energy profile represented in Figure 1: *i)* the first nucleophilic attack of carbene isocyanide **1** on DMAD **2** is the rate-determining step (RDS) of this domino process; *ii)* intermediate *trans*-**IN** quickly isomerises to *cis*-**IN**, which is 2.4 kcal/mol more stable and whose *cis* disposition is required for the following cycloaddition reaction with acetone **3** to occur; *iii)* the activation Gibbs free energy of the cycloaddition reaction of intermediate *cis*-**IN** with acetone **3** *via* **TS2** is 6.3 kcal/mol lower than that of the RDS of the domino process *via* **TS1**; *iv)* the strong exergonic character of the cycloaddition reaction between *cis*-**IN** and acetone **3** makes this process irreversible; and *v*) although the formation of intermediate *cis*-**IN** is slightly endergonic, as soon as it is formed it is quickly and irreversibly captured by acetone **3** yielding 2-imino-furan **4**. Accordingly, the MC reaction between isocyanide **1**, DMAD **2** and acetone **3** is kinetically and thermodynamically very favourable.

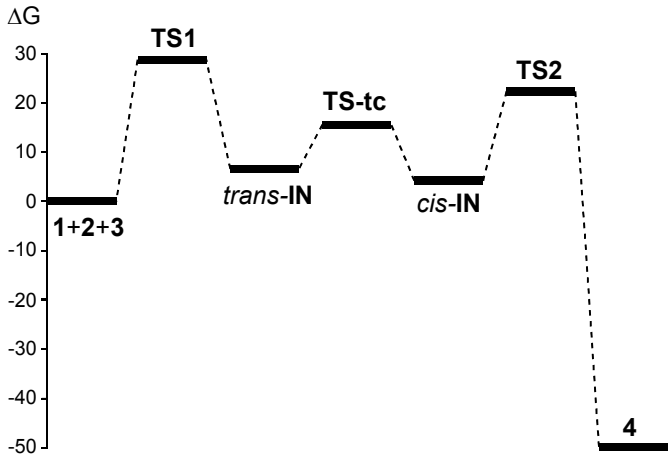

Figure 1. Gibbs free energy profile (ΔG, in kcal/mol) of the domino reaction between methyl isocyanide **1**, DMAD **2** and acetone **3**.

The geometries of the TSs involved in the domino reaction between methyl isocyanide **1**, DMAD **2** and acetone **3** in acetonitrile are shown in Figure 2. At **TS1**, associated with the nucleophilic addition of methyl isocyanide **1** to DMAD **2**, the length of the C2−C3 forming bond is 1.973 Å, while at intermediates *trans*-**IN** and *cis*-**IN** the length of the formed C2−C3 single bond is 1.407 Å. At **TS2**, associated with the cycloaddition reaction of *cis*-**IN** with acetone **3**, the lengths of the C4−C5 and C2−O6 forming bonds are 2.147 and 2.556 Å. The IRC from **TS2** towards the final 2-imino-furan **4** indicates that the second reaction of this MC process is associated with a *two-stage one-step* mechanism[36] in which the C4−C5 single bond is completely formed before the formation of the second C2−O6 single bond starts (see later). In addition, this IRC also shows that the carbonyl C5−O6 bond of acetone **3** approaches to intermediate *cis*-**IN** in the C2−C3−C4 plain, in which the two C4−C5 and C2−O6 single bonds will be formed (see **TS2** in Figure 2). This approach mode is different to that demanded in 1,3-dipolar cycloadditions, in which the dipolarophile approaches over the plain of the 1,3-dipole.

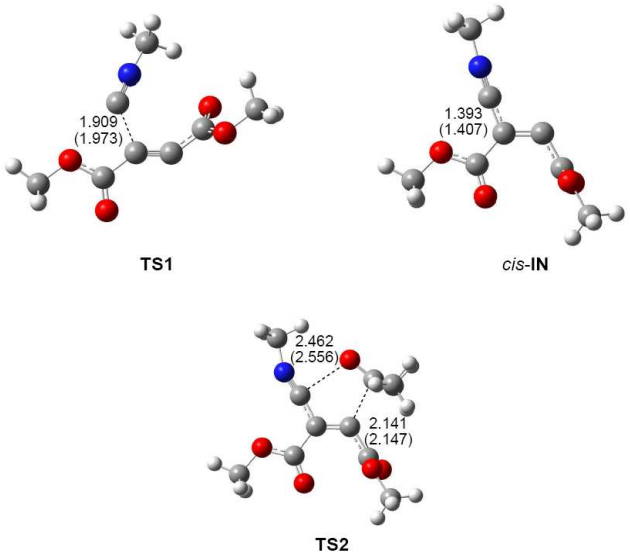

Figure 2. MPWB1K/6-311G(d,p) geometries of the most important stationary points involved in the domino reaction between methyl isocyanide **1**, DMAD **2** and acetone **3**. Distances are given in Angstroms. Lengths in acetonitrile are given in parenthesis.

The electronic nature of the nucleophilic addition reaction of carbene isocyanide **1** with DMAD **2**, as well as the cycloaddition reaction of intermediate *cis*-**IN** with acetone **3**, were analysed by computing the global electron-density transfer (GEDT).[37] The natural atomic charges, obtained through a natural population analysis (NPA), were shared between the two frameworks involved in these addition reactions. Thus, the GEDT that fluxes from the carbene isocyanide framework toward the acetylene derivative along the first reaction is 0.26e at **TS1** and 0.62e at *trans*-**IN**, indicating that along the nucleophilic addition of isocyanide **1** to DMAD **2** there is an increase of the GEDT until reaching the maximum value with the formation of the C2−C3 single bond at intermediate *trans*-**IN**. On the other hand, the GEDT that fluxes from intermediate *cis*-**IN** to the ketone framework along the second process is 0.26e at **TS2**, showing the polar character of the cycloaddition reaction between *cis*-**IN** and acetone **3**. The GEDT values calculated at both reactions emphasise the polar nature of the MC reaction between methyl isocyanide **1**, DMAD **2** and acetone **3**.

*ii) Analysis of the global and local DFT reactivity indices at the ground state of the reagents and of intermediate cis-**IN**.*

Studies devoted to polar organic reactions have shown that the analysis of the reactivity indices defined within conceptual DFT is a powerful tool to understand the reactivity in polar cycloadditions.[10] Global DFT indices, namely, the electronic chemical

potential μ, chemical hardness η, global electrophilicity ω and nucleophilicity *N*, of methyl isocyanide **1**, DMAD **2**, acetone **3** and intermediate *cis*-**IN** are given in Table 3.

Table 3. MPWB1K/6-311G(d,p) electronic chemical potential μ, chemical hardness η, global electrophilicity ω and nucleophilicity *N*, in eV, of methyl isocyanide **1**, DMAD **2**, acetone **3** and intermediate *cis*-**IN**.

	μ	η	ω	*N*
DMAD **2**	−5.01	8.95	1.40	0.91
cis-**IN**	−3.58	6.03	1.06	3.80
Acetone **3**	−3.72	9.02	0.77	2.16
Methyl isocyanide **1**	−3.90	11.46	0.66	0.77
Acetylene **5**	−3.53	11.34	0.55	1.20

The electronic chemical potential of carbene isocyanide **1**, μ = −3.90 eV, is higher than that of DMAD **2**, μ = −5.01 eV, indicating that along a polar reaction the GEDT[33] will flux from the carbene isocyanide framework towards the electron-deficient acetylene one. In the same way, the higher electronic chemical potential of intermediate *cis*-**IN**, μ = −3.58 eV, than that of acetone **3**, μ = −3.72 eV, suggests that along the subsequent cycloaddition reaction between intermediate *cis*-**IN** and acetone **3**, the GEDT will flux towards the ketone framework.

Methyl isocyanide **1** presents an electrophilicity ω index of 0.66 eV and a nucleophilicity *N* index of 0.77 eV, being classified on the borderline of moderate electrophiles[38] and as a marginal nucleophile.[39] Accordingly, carbene isocyanide **1** is considered a weak nucleophile participating in polar reactions and, therefore, a strongly electrophilically activated molecule will be necessary to make the nucleophilic attack of methyl isocyanide **1** feasible.

Polar organic reactions require the participation of good electrophiles and good nucleophiles. Acetylene **5** is one of the poorest electrophilic, ω = 0.55 eV, and nucleophilic, *N* = 1.20 eV, species involved in polar organic reactions, being classified as a marginal electrophile and a marginal nucleophile. Therefore, it cannot participate in polar reactions. Inclusion of two methyl carboxylate groups in the acetylene framework drastically increases the electrophilicity ω index of DMAD **2**, ω = 1.40 eV, being classified as a strong electrophile, and slightly decreases its nucleophilicity *N* index to *N* = 0.91 eV, remaining classified as a marginal nucleophile. In spite of the strong electrophilic character of DMAD **2**, the low nucleophilic character of isocyanide **1**

accounts for the high activation energy associated with the nucleophilic addition of isocyanide **1** to DMAD **2** (see above).

Otherwise, the electrophilicity ω and nucleophilicity *N* indices of intermediate *cis*-**IN**, ω = 1.06 eV and *N* = 3.80 eV, allow its classification on the borderline of strong electrophiles and as a strong nucleophile. Acetone **3**, which presents an electrophilicity ω index of ω = 0.77 eV and a nucleophilicity *N* index of *N* = 2.16 eV, will behave as a moderate electrophile and a moderate nucleophile. It is interesting to remark that the low electrophilic character of acetone **3** demands its electrophilic activation in order to participate in polar reactions.

Recently, the electrophilic P_k^+ and nucleophilic P_k^- Parr functions have been proposed to analyse the local reactivity in polar processes[28] involving reactions between a nucleophile/electrophile pair. Accordingly, the electrophilic P_k^+ Parr functions for DMAD **2** and acetone **3**, and the nucleophilic P_k^- Parr functions for methyl isocyanide **1** and intermediate *cis*-**IN** are analysed (see Figure 3).

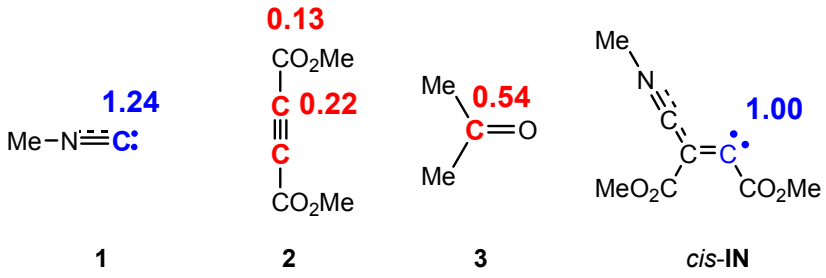

Figure 3. Nucleophilic P_k^- Parr functions, in blue, and electrophilic P_k^+ Parr functions, in red, in methyl isocyanide **1**, DMAD **2**, acetone **3** and intermediate *cis*-**IN**.

The analysis of the nucleophilic P_k^- Parr functions of carbene isocyanide **1** and *cis*-**IN** shows that the C2 carbon of isocyanide **1** and the C4 carbon of intermediate *cis*-**IN** present the maximum values, P_k^- = 1.24 and 1.00, respectively, indicating that these sites are the most nucleophilic centers of these species (see Scheme 4 for atom numbering). From these values two appealing conclusions can be obtained: *i)* carbene isocyanide **1** experiences a strong nucleophilic activation at the C2 carbon; and *ii)* at nucleophilic intermediate *cis*-**IN**, the nucleophilic P_k^- Parr functions are concentrated at the C4 carbon. The strong nucleophilic activation at the C2 carbon of isocyanide **1** is a consequence of the nucleophilic deactivation of the N1 nitrogen atom.

On the other hand, analysis of the electrophilic P_k^+ Parr functions of DMAD **2** indicates that the acetylene C3 and C4 carbons, P_k^+ = 0.22, are *ca.* twice as electrophilically activated as the carbonyl carbons, P_k^+ = 0.13. Finally, acetone **3** presents its electrophilic activation at the carbonyl carbon atom, $P_k^+ = 0.54$.

Consequently, the most favourable electrophile-nucleophile interaction along the nucleophilic attack of carbene isocyanide **1** on DMAD **2** will take place between the most nucleophilic center of isocyanide **1**, the C2 carbon, and the most electrophilic center of DMAD **2**, the C3 or C4 carbon. Likewise, the most favourable bond formation along the nucleophilic attack of intermediate *cis*-**IN** on acetone **3** will take place between the most nucleophilic center of the former, the C4 carbon, and the electrophilic carbon atom of acetone **3**.

*iii) BET analysis of the domino reaction between methyl isocyanide **1**, DMAD **2** and acetone **3**.*

Several theoretical studies have shown that the ELF topological analysis of the changes of electron-density, ρ(**r**), along a reaction path can be used as a valuable tool to understand the bonding changes along the reaction path, and consequently to establish the molecular mechanisms.[29] After an analysis of the electron-density, ELF provides basins of attractors, which are the domains in which the probability of finding an electron pair is maximal.[40] The spatial points in which the gradient of ELF has a maximum value are designated as attractors. The basins are classified as core basins and valence basins. The latter are characterised by the synaptic order, *i.e.* the number of atomic valence shells in which they participate. Thus, there are monosynaptic, disynaptic, trisynaptic basins and so on.[41] Monosynaptic basins, labelled V(A), correspond to the lone pairs or non-bonding regions, while disynaptic basins, labelled V(A,B), connect the core of two nuclei A and B and, thus, correspond to a bonding region between A and B. This description recovers the Lewis bonding model, providing a very suggestive graphical representation of the molecular system.

ELF topological analysis of the structures involved in an elementary step allows characterising mainly three types of valence basins: *i)* protonated basins, V(A,H); *ii)* monosynaptic basins, V(A), associated with lone pairs or non-bonding regions; and *iii)* disynaptic basins, V(A,B), associated with bonding regions. A set of ELF valence

basins topologically characterises a molecular structure. Analysis of changes in number or type of valence basins of the structures involved along the IRC of the reaction allows establishing a set of points, **Pi**, defining the different phases that topologically characterise a molecular mechanism. The further analysis of the different phases characterised by these significant points permits its characterisation.[31]

Herein, a BET study of the MC reaction between isocyanide **1**, DMAD **2** and acetone **3** is performed in order to gain insight into how the bonding changes take place along this domino reaction, and thus, to establish the molecular mechanism of the two consecutive reactions.

*iii.a) BET study of the nucleophilic addition reaction of methyl isocyanide **1** with DMAD **2**.*

The BET study of the nucleophilic addition reaction of carbene methyl isocyanide **1** to DMAD **2** indicates that this reaction is topologically characterised by six differentiated phases. The population of the most significant valence basins of the selected points of the IRC is included in Table 4. The attractor positions of the ELF for the relevant points along the IRC are shown in Figure 4, while the basin-population changes along the reaction path are graphically represented in Figure 5.

Phase I, 3.73 Å ≥ d(C2−C3) > 2.28 Å, begins at molecular complex **MC1**, d(C2−C3) = 3.726 Å, being a minimum in the PES connecting **TS1** with the separated reagents **1** and **2**. The ELF picture of **MC1** exhibits the topological characteristics of the separated reagents. ELF analysis of **MC1** shows two V(N1,C2) and V'(N1,C2) disynaptic basins with a population of 3.81e and 1.29e, associated with the N1≡C2 triple bond region of the isocyanide framework, and one V(C2) monosynaptic basin integrating 2.65e related to the C2 carbon lone pair. In addition, ELF topology of **MC1** also shows the presence of two V(C3,C4) and V'(C3,C4) disynaptic basins with populations of 2.41e and 2.46e belonging to the C3≡C4 triple bond of the acetylene framework.

Phase II, 2.28 Å ≥ d(C2−C3) > 2.03 Å, starts at **P1**. The first noticeable topological change along the IRC occurs in this phase; a new V(C4) monosynaptic basin, integrating 0.53e, is created at **P1**. The electron-density of this basin mainly proceeds from the depopulation of the C3≡C4 triple bond region until V(C3,C4) and V'(C3,C4) disynaptic basins reach a total population of 4.85e. Note that the new V(C4)

monosynaptic basin is associated with the non-bonding sp^2 hybridised lone pair present at the C4 carbon of nucleophilic intermediate *cis*-**IN**. On the other hand, the population of the V(C2) monosynaptic basin slightly decreases. GEDT has increased to a small extent, 0.07e.

Phase III, 2.03 Å ≥ d(C2−C3) > 1.90 Å, begins at **P2**. At this point, the two V(N1,C2) and V'(N1,C2) disynaptic basins present at **MC1** have merged into a new V(N1,C2) disynaptic basin integrating 5.12e. This topological change simply is the consequence of electron-density redistribution in the N1−C2 bonding region. In this phase, the TS of the reaction, **TS1**, d(C2−C3) = 1.909 Å, is found. At this structure, only scanty changes in the electron-density distribution with respect to those found at **P1** are observed with the exception that the population of the V(C4) monosynaptic basin has increased to 1.06e. GEDT has increased to 0.18e.

At *phase IV*, 1.90 Å ≥ d(C2−C3) > 1.55 Å, which begins at **P3**, the most significant topological change along the reaction path takes place. The V(C2) monosynaptic basin present at **P2** is converted into a new V(C2,C3) disynaptic basin with an initial population of 2.55e (see **P2** and **P3** in Figure 4 and the change from V(C1), in green in **P2**, to V(C2,C3), in blue in **P3**, in Figure 5). In spite of the unexpected position of the V(C1) ELF attractor, the depiction of the valence basins associated with **P3** shows the disynaptic character of the corresponding basin (see **P3** in Figure 4). This relevant topological change indicates that the formation of the new C2−C3 single bond has already begun at a distance of 1.90 Å with a high electron-density population. In addition, the V(C4) monosynaptic basin increases its population to 1.31e together with the decrease of the total population of V(C3,C4) and V'(C3,C4) disynaptic basins to 4.12e, which indicates that the C3−C4 bonding region has just acquired its double bond character. At **P3**, the GEDT is 0.27e.

Phase V, 1.55 Å ≥ d(C2−C3) > 1.40 Å, starts at **P4**. At this point a new V(N1) monosynaptic basin appears with a population of 0.66e as the consequence of the depopulation of the V(N1,C2) disynaptic basin to 4.71e. The electron-density of the V(C3,C4) and V'(C3,C4) disynaptic basins continues to decrease until reaching a population of 3.47e, while the V(C4) monosynaptic basin has increased to 1.75e. The GEDT strongly increases to 0.54e.

Finally, the extremely short *phase VI*, 1.40 Å ≥ d(C2−C3) ≥ 1.39 Å, begins at **P5** and ends at nucleophilic intermediate *trans*-**IN**, d(C2−C3) = 1.396 Å. At **P5**, the two

V(C3,C4) and V'(C3,C4) disynaptic basins merge into one V(C3,C4) disynaptic basin integrating 3.10e, whereas the V(C4) monosynaptic basin has received almost the population of a lone pair, 1.90e. Besides, while the V(N1,C2) disynaptic basin decreases by 0.31e, the V(N1) monosynaptic and V(C2,C3) disynaptic basins increase their populations to 1.20e and 2.73e, respectively. At **P5**, the maximum GEDT along the reaction takes place, 0.60e. From **P5** to *trans*-**IN**, the most noticeable topological change is the disappearance of the V(N1) monosynaptic basin simultaneously with the strong increase of the population of the V(N1,C2) disynaptic basin to 5.52e. At *trans*-**IN**, the V(C3,C4) disynaptic basin presents a population of 3.10e, indicating that the C3−C4 bonding region is very polarised towards the C2−C3 single bond created at *phase IV*, which is characterised by one V(C2,C3) disynaptic basin integrating 2.71e. At last, the V(C4) monosynaptic basin associated with the C4 carbon lone pair has a population of 1.97e. The GEDT computed at *trans*-**IN**, 0.62e, is very high.

Table 4. Valence basin populations *N* calculated from the ELF of the IRC points, P1-P5, defining the six phases characterising the molecular mechanism associated with the addition reaction between carbene isocyanide **1** and DMAD **2**. The stationary points **MC1**, *trans*-**IN** and *cis*-**IN** are also included. Distances are given in Å, while the GEDTs obtained by NPA analysis are given in e.

Phases		*I*	*II*	*III*	*IV*	*V*	*VI*	
	MC1	**P1**	**P2**	**P3**	**P4**	**P5**	*trans*-**IN**	*cis*-**IN**
d(C2−C3)	3.726	2.282	2.033	1.897	1.551	1.399	1.396	1.393
GEDT	0.00	0.07	0.18	0.27	0.54	0.60	0.62	0.65
V(N1,C2)	3.81	3.15	5.12	5.13	4.71	4.40	5.52	3.19
V'(N1,C2)	1.29	2.00						2.32
V(C3,C4)	2.68	2.37	2.23	2.10	1.73	3.10	3.13	3.14
V'C3,C4)	2.65	2.48	2.16	2.02	1.74			
V(C2)	2.65	2.58	2.52					
V(C2,C3)				2.55	2.66	2.73	2.71	2.65
V(C4)		0.52	1.06	1.31	1.75	1.90	1.97	2.06
V(N1)					0.66	1.20		

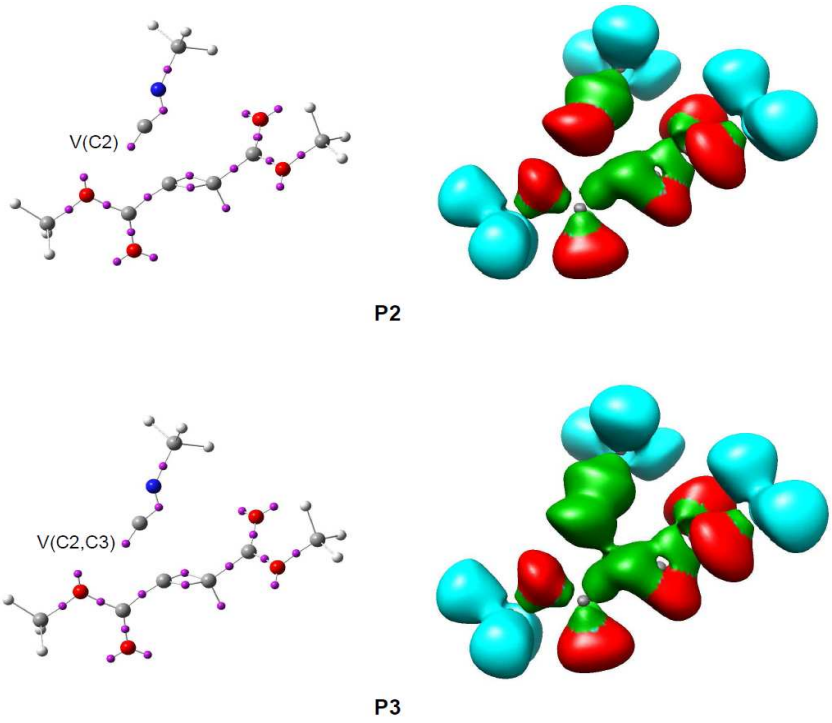

Figure 4. ELF attractor positions and basins for the most relevant points along the IRC associated with the formation of the C2−C3 single bond along the nucleophilic addition reaction of methyl isocyanide **1** with DMAD **2**. Disynaptic basins are coloured in green and monosynaptic basins are in red.

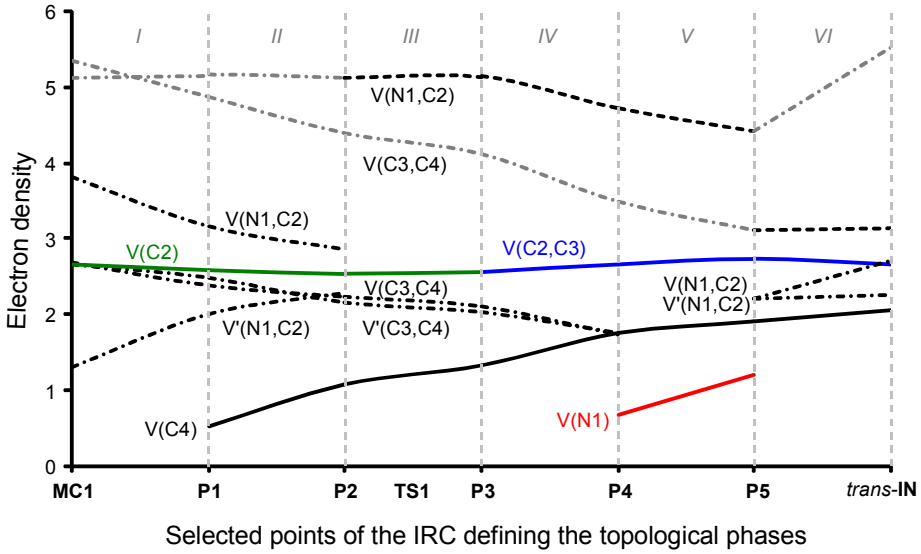

Figure 5. Graphical representation of the basin population changes along the cycloaddition reaction between methyl isocyanide **1** and DMAD **2**. Point dotted curves in grey represent the sum of disynaptic basins describing a bond region or monosynaptic basins describing lone pairs.

*iii.b) BET study of the reaction between intermediate cis-**IN** and acetone **3**.*

The study of the nucleophilic attack of intermediate *cis*-**IN** on acetone **3** shows that this reaction can be topologically characterised by eight differentiated phases. The populations of the most significant valence basins of the selected points of the IRC are compiled in Table 5. The attractor positions of the ELF for relevant points along the IRC are shown in Figure 6, while the basin population changes along the reaction path are graphically represented in Figure 7.

Phase I, 3.69 Å ≥ d(C4−C5) > 2.80 Å and 3.09 Å ≥ d(C2−O6) > 3.00 Å, begins at molecular complex **MC2**, d(C4−C5) = 3.687 Å and d(C2−O6) = 3.090 Å, which is a minimum in the PES connecting intermediate *cis*-**IN** and acetone **3** with the corresponding **TS2**. The ELF picture of **MC2** shows the topological behaviour of the separated reagents. Three disynaptic basins, V(N1,C2), V(C2,C3) and V(C3,C4) integrating 5.50e, 2.60e and 3.17e, respectively, can be observed, which are associated with the N1−C2−C3−C4 bonding region of intermediate *cis*-**IN**. The most important characteristic on this framework is the presence of one V(C4) monosynaptic basin with a population of 2.05e, which is associated with a non-bonding sp^2 hybridised lone pair present in the C4 carbon. On the other hand, ELF analysis of **MC2** also shows the presence of two monosynaptic basins, V(O6) and V'(O6), with a population of 2.64e and 2.64e, associated with the O6 oxygen lone pairs, and one V(C5,O6) disynaptic basin integrating 2.39e which belong to the C−O bonding region of acetone **3**. The low population of the C−O bond together with the high population of the oxygen lone pairs indicate that the C−O bond of acetone **3** is very polarised.

Phase II, 2.80 Å ≥ d(C4−C5) > 2.33Å and 3.00 Å ≥ d(C2−O6) > 2.62 Å, begins at **P1**. At this phase the most relevant changes imply the splitting of the V(N1,C2) disynaptic basin into two V(N1,C2) and V'(N1,C2) disynaptic basins with a population of 1.78e and 3.70e, and a slight decrease in the population of the V(C4) monosynaptic basin to 2.00e. The other basins maintain their populations as shown at *phase I*. Along this phase, the population of the V(C4) monosynaptic basin slightly decreases to 2.00e. On the acetone framework, the population of the V(C5,O6) disynaptic basin is 2.41e, while the two V(O6) and V'(O6) monosynaptic basins integrate 2.65e and 2.70e, respectively.

Phase III, 2.34 Å ≥ d(C4−C5) > 2.14 Å and 2.62 Å ≥ d(C2−O6) > 2.46 Å, begins at **P2**. At this point, the V(N1,C2) and V'(N1,C2) disynaptic basins newly merge into

one disynaptic basin V(N1,C2) integrating 5.58e, while the population of V(C4) monosynaptic basin has slightly decreased to 1.92e on the *cis*-**IN** moiety. The populations of the V(O6) and V'(O6) monosynaptic basins slightly increase to 2.71e and 2.77e at the acetone framework. These changes can be related to the GEDT that fluxes from *cis*-**IN** to acetone **3** along this polar reaction.

Phase IV, 2.14 Å ≥ d(C4−C5) > 2.07 Å and 2.46 Å ≥ d(C2−O6) > 2.41 Å, begins at **P3**, which corresponds to the TS of the reaction, **TS2**, d(C4−C5) = 2.141 Å and d(C2−O6) = 2.462 Å. At this point, the first most relevant change along the IRC is found; while the V(C4) monosynaptic basin present in *cis*-**IN** has disappeared, a new V(C4,C5) disynaptic basin, integrating 1.87e, has appeared (see **P2** and **P3** in Figure 6 and the change from V(C4), in green in **P2**, to V(C4,C5), in blue in **P3**, in Figure 7). This change indicates that the formation of the new C4−C5 single bond has started at d(C4−C5) = 2.14 Å.

Phase V, 2.07 Å ≥ d(C4−C5) > 1.91 Å and 2.41 Å ≥ d(C2−O6) > 2.29 Å, starts at the **P4**. After passing **TS2**, the most important change is the formation of a new V(N1) monosynaptic basin, which integrates 0.80e, together with the depopulation of the V(N1,C2) disynaptic basin to 4.75e. At this point, the V(C3,C4) disynaptic basin present in *cis*-**IN** splits into two disynaptic basins, V(C3,C4) and V'(C3,C4), integrating 1.68e and 1.61e, respectively. In addition, the population of the V(C4,C5) disynaptic basin slightly increases to 1.89e, as well as the populations of the V(O6) and V'(O6) monosynaptic basins of the acetone framework to 2.82e and 2.87e.

Phase VI, 1.91 Å ≥ d(C4−C5) > 1.65Å and 2.29 Å ≥ d(C2−O6) > 2.14 Å, starts at the **P5**. At this point, the V(N1,C2) disynaptic basin of the intermediate moiety newly splits into two V(N1,C2) and V'(N1,C2) disynaptic basins, which integrate 2.14e and 2.09e, respectively, while the V(N1) monosynaptic basin reaches a population of 1.48e. On the acetone moiety, it may be seen a depopulation of the V(C5,O6) disynaptic basin to 1.77e and a slight increase of the population of the V(O6) and V'(O6) monosynaptic basins to 2.94e and 2.96e.

The short *phase VII,* 1.65 Å ≥ d(C4−C5) > 1.58 Å and 1.95 Å ≥ d(C2−O6) > 1.75 Å, starts at **P6**. At this point, the second relevant topological change along the IRC takes place: a V(C2) monosynaptic basin is created at the C2 carbon integrating 0.20e (see the V(C2) monosynaptic basin in **P6** in Figure 6). This change shows the preparation of the intermediate fragment for the subsequent ring closure through the C−O bond formation.

At this phase, the population of the V(C4,C5) disynaptic basin increases to 2.05e and the population of the V(N1) monosynaptic basin increases to 2.26e, whereas the populations of the V(C5,O6), V(N1,C2) and V'(N1,C2) disynaptic basins decrease to 1.53e, 1.83e and 1.84e, respectively, along the reaction progress.

Phase VIII, 1.58 Å ≥ d(C4−C5) ≥ 1.50 Å and 1.75 Å ≥ d(C2−O6) ≥ 1.37 Å, starts at **P7** and ends at cycloadduct **4**, d(C4−C5) = 1.502 Å and d(C2−O6) = 1.370 Å. At this point, the third most relevant change takes place with the formation of a new V(C2,O6) disynaptic basin integrating 0.75e (see the V(C2,O6) disynaptic basin in **P7** in Figure 6 and the change from V(C2), in green in **P6**, to V(C2,O6), in blue in **P7**, in Figure 7), while the populations of the V(O6) and V'(O6) monosynaptic basins have slightly decreased to 2.71e and 2.69e. This change indicates that the formation of the second C2−O6 single bond has started at a distance of 1.75 Å. At 2-imino-furan **4**, the V(C2,O6) disynaptic basin reaches a population of 1.49e, while the V(C4,C5) disynaptic basin shows a population of 2.09e. The low population of the V(C2,O6) disynaptic basin indicates a very polarised C2−O6 single bond.

Table 5. Valence basin populations *N* calculated from the ELF of the IRC points, P1-P7, defining the eight phases characterising the molecular mechanism associated with the cycloaddition reaction between nucleophilic intermediate *cis*-**IN** and acetone **3**. The stationary points **MC2** and **4** are also included. Distances are given in Å, while the GEDTs obtained by NPA analysis are given in e.

Phases	*I*	*II*	*III*	*IV*	*V*	*VI*	*VII*	*VIII*	
	MC2	**P1**	**P2**	**P3**	**P4**	**P5**	**P6**	**P7**	**4**
d(C4−C5)	3.687	2.798	2.338	2.141	2.070	1.908	1.645	1.578	1.502
d(C2−O6)	3.090	3.007	2.623	2.462	2.412	2.288	1.953	1.746	1.370
GEDT	0.00	0.04	0.16	0.26	0.31	0.40	0.39	0.32	0.19
V(N1,C2)	5.50	1.78	5.48	5.53	4.75	2.14	1.83	1.72	1.64
V'(N1,C2)		3.70				2.09	1.84	1.74	1.63
V(N1)					0.8	1.48	2.26	2.48	2.67
V(C2,C3)	2.60	2.63	2.6	2.59	2.61	2.6	2.47	2.39	2.34
V(C3,C4)	3.17	3.16	3.24	3.27	1.68	1.64	1.71	1.73	1.73
V'(C3,C4)					1.61	1.68	1.68	1.68	1.69
V(O6)	2.64	2.65	2.71	2.85	2.82	2.94	2.92	2.71	2.24
V'(O6)	2.64	2.70	2.77	2.81	2.87	2.96	2.99	2.69	2.52
V(C5,O6)	2.39	2.41	2.23	2.18	2.06	1.77	1.53	1.41	1.43
V(C4)	2.05	2.00	1.92						
V(C4,C5)				1.87	1.89	1.94	2.05	2.06	2.09
V(C2)							0.20		
V(C2,O6)								0.75	1.49

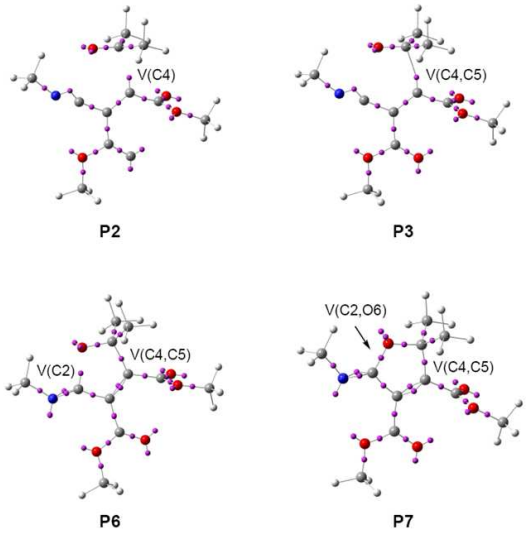

Figure 6. ELF attractor positions for the most relevant points along the IRC associated with the formation of the C4−C5 and C2−O6 single bonds along the cycloaddition reaction of intermediate *cis*-**IN** with acetone **3**.

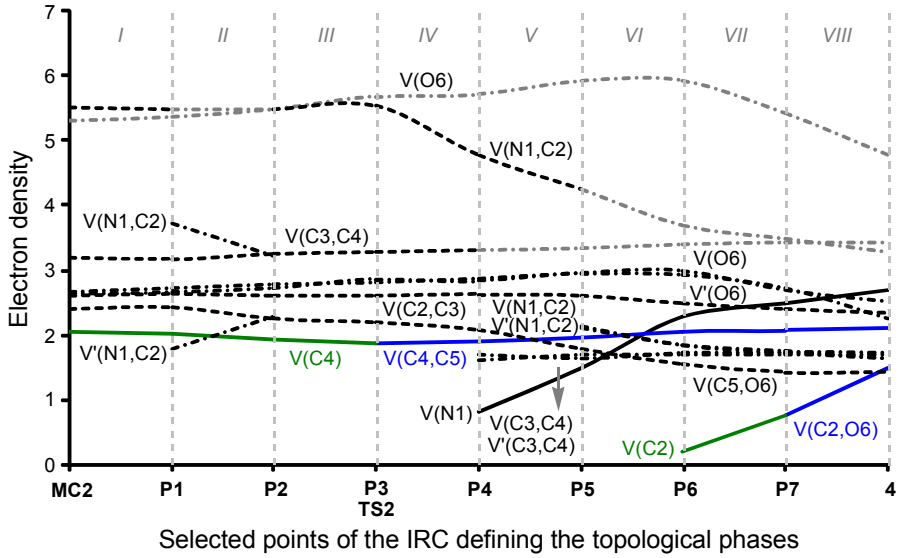

Figure 7. Graphical representation of the basin population changes along the cycloaddition reaction between nucleophilic intermediate *cis*-**IN** and acetone **3**. Point dotted curves in grey represent the sum of disynaptic basins describing a bond region or monosynaptic basins describing lone pairs.

From the BET analysis of this domino reaction some appealing conclusions can be drawn: *i)* along the nucleophilic attack of methyl isocyanide **1** on DMAD **2**, the C2−C3 bond is formed at a distance of 1.90 Å through the donation of the electron-density of the carbene C2 lone pair to one of the two acetylenic carbons of DMAD **2**; *ii)* the formation of the new C2−C3 bond takes place with a high electron-density, 2.55e. Note that this value is higher than that associated with a C−C single bond; *iii)* along the nucleophilic attack of isocyanide **1** on DMAD **2**, a new V(C4) monosynaptic basin with an initial population of 0.52e appears at the C4 carbon as the consequence of the depopulation of the acetylenic C3−C4 bonding region. This V(C4) monosynaptic basin reaches a population of 2.06e at intermediate *cis*-**IN**, while at the same time the C3−C4 bonding region is depopulated to reach 3.14e; *iv)* along the nucleophilic attack of *cis*-**IN** on acetone **3**, the formation of the C4−C5 single bond begins at a distance of 2.14 Å through the donation of the electron-density of the carbenoid C4 lone pair of *cis*-**IN** to the carbonyl C5 carbon of acetone **3**; *v*) formation of the second C2−O6 single bond takes place at the end of the cycloaddition path at a distance of 1.75 Å by sharing the

electron-density of the V(C2) monosynaptic basin present at the C2 carbon and some electron-density of the V(O6) monosynaptic basins associated with the oxygen O6 lone pairs; *vi*) formation of the C2−O6 single bond begins after the complete formation of the C4−C5 one, characterising the mechanism of the cycloaddition as a non-concerted *two-stage one-step* mechanism; and finally vii) along the cycloaddition step, the N1≡C2 triple bond of *cis*-**IN** becomes a double bond characterised by the presence of two V(N1,C2) and V'(N1,C2) disynaptic basins at imino-furan **4**. At the same time, the C2 carbon is rehybridised from sp at *cis*-**IN** to sp^2 at imino-furan **4** as a consequence of the formation of the C2−O6 single bond. The orthogonal character of the new C2−O6 single bond with respect to the exocyclic N1−C2 double bond present in imino-furan **4** indicates that the N1−C2 triple bond and C3−C4 double bond regions of intermediate *cis*-**IN** do not participate directly in the cycloaddition reaction, as expected in a 1,3-dipole participating in a 1,3-dipolar cycloaddition.

Both analysis of the atomic movements of the *cis*-**IN** and acetone **3** molecules along the IRC associated with the cycloaddition step and the corresponding BET analysis indicate that the electron-density of the carbenoid C4 carbon and the carbonyl O6 oxygen lone pairs mainly participate in the formation of the C4−C5 and C2−O6 single bonds along the reaction; consequently, this cycloaddition should be classified as a [2n+2n], in which only two lone pairs are involved, and not as a [4π+2π] in a 1,3-dipolar cycloaddition.

*iv) What is the electronic structure of intermediate cis-**IN** and the origin of the high reactivity of carbonyl compounds towards this intermediate?*

At first, intermediate *cis*-**IN** can be represented by either of the Lewis resonant structures **A** and **B** given in Scheme 5. Both structures would represent a zwitterionic intermediate in which the negative charge is located at the C4 carbon atom, while the positive charge can be located at the C2 or N1 atoms belonging to the methyl isocyanide framework. Experimental chemists represent *cis*-**IN** by means of the 1,3-zwitterionic structure **A**, since it justifies the participation of *cis*-**IN** in a [3+2] cycloaddition toward carbonyl derivatives.

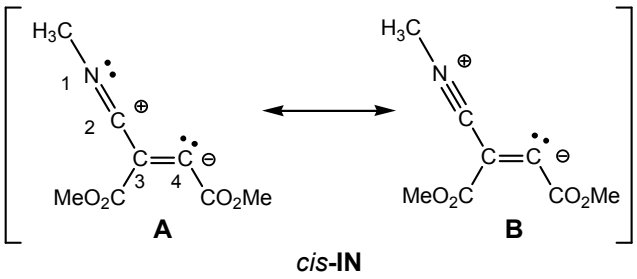

Scheme 5. Lewis structures representing zwitterionic intermediate *cis*-**IN**.

Both NPA and ELF analyses of the electronic structure of the intermediate *cis*-**IN** yield a different representation for this intermediate. NPA analysis of *cis*-**IN** clearly shows the zwitterionic character of this intermediate: while the methyl isocyanide framework is positively charged, the DMAD framework is negatively charged (see Figure 8a). However, while NPA indicates that the positive charge is mainly located at the C2 carbon, in agreement with Lewis structure **A**, the results also indicate that the negative charge is mainly located at the C3 carbon and the carboxylate oxygen atoms, the C4 carbon having a negligible negative charge of −0.07e.

On the other hand, ELF topology of *cis*-**IN** shows the presence of a monosynaptic basin at C4, V(C4), integrating 2.07e (see Figure 8b). In addition, the C3−C4 double bond regions of Lewis structures **A** and **B** have a noticeable depopulation, 3.14e. This behaviour can account for the negligible negative charge found at the C4 carbon, −0.07e, thus both Lewis structures, **A** and **B,** can be ruled out to represent intermediate *cis*-**IN**.

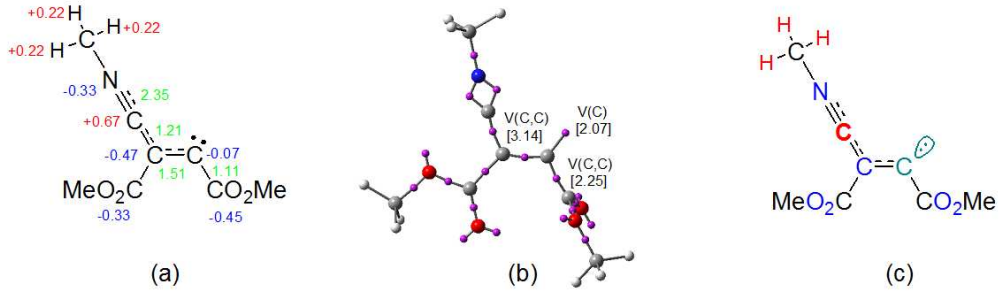

Figure 8. Electronic representation of the structure of carbenoid intermediate *cis*-**IN** based on (a) NPA, (b) ELF and (c) the mixture of both analyses. Green values in (a) indicate the bond order of the corresponding bond.

Consequently, in spite of the zwitterionic character of intermediate *cis*-**IN**, it appears that the reactivity of this intermediate towards carbonyl compounds cannot be

related to its zwitterionic character but rather to the singlet carbenoid character of the C4 carbon that grants a high nucleophilic character to this molecule (see the C4 carbon in green in Figure 8c).

In order to explain the high reactivity of acetone **3** towards this intermediate, an analysis of the molecular electrostatic potential (MEP) at *cis*-**IN** and the corresponding **TS2** was also performed (see Figure 9). MEP of *cis*-**IN** allows reaching two appealing conclusions: *i)* around the nucleophilic C4 carbon a low negative electrostatic potential (in red) is found (see Figure 9a). Note that the carboxylate oxygen atoms show the highest values. This behaviour is in agreement with the unappreciable negative charge found at the C4 atom; *ii)* interestingly, the region of MEP with the highest positive value of *cis*-**IN** corresponds to the methyl substituent present in the isocyanide framework.

MEP of carbenoid intermediate *cis*-**IN** shows the special characteristic of this intermediate that favours the nucleophilic attack on carbonyl derivatives. As can be seen in Figure 9, the analysis of the MEP of **TS2** clearly shows that along the nucleophilic attack of *cis*-**IN** on acetone **3**, the GEDT that takes place in this polar process gives rise to an increase of electron-density of the oxygen carbonyl atom. This feature, which is unfavourable in an uncatalysed nucleophilic addition to carbonyl compounds, is favoured in **TS2** by the presence of the positively charged methyl group that electrostatically stabilises the negative charge developed at the carbonyl oxygen atom (see Figure 9b). Note that along the formation of the first C4−C5 single bond, the GEDT that takes place from *cis*-**IN** to acetone **3**, 0.40e at **P5**, mainly locates the electron-density at the carbonyl oxygen atom (see the integration of the V(O6) and V'(O6) monosynaptic basins at **P5** in Table 5).

Finally, in order to rule out a stabilisation of **TS2** by a hydrogen bond between the carbonyl oxygen atom and one hydrogen atom of the methyl group, an analysis of the NCI at **TS2** was performed. As can be seen in Figure 9c, although some weak interactions between the carbonyl oxygen atom and the methyl isocyanide framework appear (in green), no hydrogen bond interaction between the carbonyl oxygen and the hydrogen of the methyl group is observed. Note that strong hydrogen bonds appear as a dark turquoise surface. Indeed, the NCI between the carbonyl O6 oxygen atom and the C2 carbon of the isocyanide framework is stronger than that involving the hydrogen of the methyl group, indicating the favourable interaction preceding the C2−O6 single bond formation.

Consequently, we can conclude that the high reactivity of intermediate *cis*-**IN** towards carbonyl derivatives is due to two specific features: *i)* the carbenoid character of the sp^2 hybridised C4 carbon more than the negative charge on a carbanionic center and, *ii)* the special geometric disposition of the alkyl substituents in isocyanides that electrostatically favours the GEDT along the nucleophilic attack of these carbenoid intermediates on carbonyl compounds.

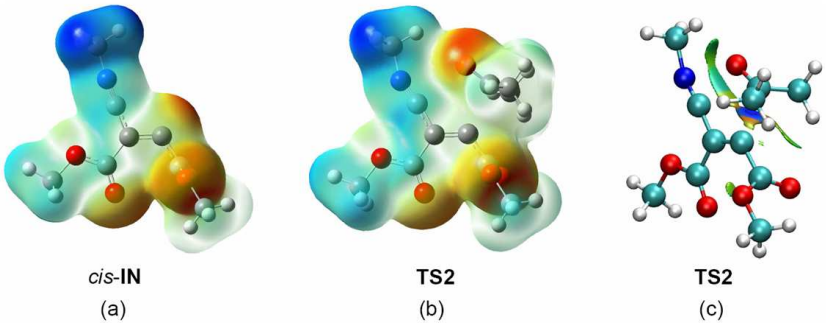

Figure 9. MEP of carbenoid intermediate *cis*-**IN** (a) and **TS2** (b), and NCIs at **TS2** (c).

Conclusions

The high reactivity of acetone **3** towards nucleophilic carbenoid intermediate *cis*-**IN**, generated *in situ* by the addition of methyl isocyanide **1** to DMAD **2**, has been studied using DFT methods at the MPWB1K/6-311G(d,p) computational level through the combination of the exploration and characterisation of the PESs associated with this MC reaction and the analysis based on the MEDT, consisting of the analysis of the reactivity indices derived from the conceptual DFT at the ground state of the reagents and the BET study along the corresponding reaction paths.

This MC reaction is a domino process that comprises two consecutive reactions: *i)* formation of carbenoid intermediate *trans*-**IN**, which quickly equilibrates with the thermodynamically more stable *cis*-**IN**; and *ii)* the nucleophilic capture of acetone **3** by carbenoid intermediate *cis*-**IN** yielding the formation of the final 2-imino-furan **4**.

Analysis of the relative Gibbs free energies in acetonitrile indicates that while the initial nucleophilic attack of carbene methyl isocyanide **1** on DMAD **2** is the RDS of this MC reaction; once intermediate *cis*-**IN** is formed it quickly and irreversibly captures acetone **3**.

Analysis of the DFT reactivity indices at intermediate *cis*-**IN** clearly accounts for its high nucleophilic character, entirely at the carbenoid C4 carbon. These behaviours explain the high reactivity of intermediate *cis*-**IN** in polar reactions towards electron-deficient carbonyl compounds.

BET analysis of the two reactions involved in this domino process makes it possible to draw some appealing conclusions concerning the bonding changes occurring in this MC reaction: *i)* along the nucleophilic attack of isocyanide **1** on DMAD **2**, the C2−C3 bond is formed at a distance of 1.90 Å through the donation of the electron-density of the carbene C2 lone pair to one of the two acetylenic carbons of DMAD. Formation of this C2−C3 bond takes place with a high electron-density, 2.55e; *ii)* along the nucleophilic attack of isocyanide **1** on DMAD **2**, a new V(C4) monosynaptic basin with an initial population of 0.52e appears at the C4 carbon as the consequence of the depopulation of the acetylenic C3−C4 triple bond. This V(C4) monosynaptic basin reaches a population of 2.06e at intermediate *cis*-**IN**; *iii)* along the nucleophilic attack of *cis*-**IN** on acetone **3**, the formation of the C4−C5 single bond begins at a distance of 2.14 Å through the donation of the electron-density of the carbenoid C4 lone pair of *cis*-**IN** on the carbonyl C5 carbon of acetone **3**; *iv*) formation of the second C2−O6 single

bond takes place at the end of the cycloaddition path at a distance of 1.75 Å by sharing the electron-density of the V(C2) monosynaptic basin present at the C2 carbon and some electron-density of the V(O6) monosynaptic basins associated with the O6 oxygen lone pairs; *v*) formation of the C2−O6 single bond begins after the complete formation of the C4−C5 one. This behaviour characterises the mechanism of the cycloaddition as a non-concerted *two-stage one-step* mechanism.[36]

An analysis of the electronic structure of intermediate *cis*-**IN** makes it posible to explain the high reactivity of this intermediate towards carbonyl derivatives. Two specific features of this intermediate enable this MC reaction: *i)* the carbenoid character of the sp^2 hybridised C4 carbon of *cis*-**IN** more than the negatively charged carbanionic center as it is represented in the bibliography; and, *ii)* the special geometric disposition of the alkyl substituent present in the isocyanide, which electronically stabilises the negative charge gathered at the carbonyl oxygen atom along the nucleophilic attack.

The present MEDT study permits establishing that the high nucleophilic character of carbenoid intermediate *cis*-**IN** together with the specific approach mode of the carbonyl C=O double bond along the nucleophilic attack of the sp^2 hybridised carbenoid center of *cis*-**IN** on the carbonyl carbon of acetone **3** make the formation of the C−C single bond with a very low activation enthalpy, 3.3 kcal/mol, possible, without any external electrophilic activation of the carbonyl group, while the geometric and electronic features of this intermediate favour the subsequent ring closure through the downhill formation of the C−O single bond, thus providing the answers to the three unresolved questions posed concerning the electronic structure of the involved intermediate and the molecular mechanism of these experimentally widely investigated MC reactions.

Finally, both the analysis of the atomic movements of the molecules *cis*-**IN** and acetone **3** along the IRC associated with the cycloaddition step and the corresponding BET analysis allow characterising the mechanism of this reaction as a [2n+2n] cycloaddition in which only two lone pairs are involved in the formation of the new C4−C5 and C2−O6 single bond. These findings make it possible to reject the 1,3-dipolar cycloaddition mechanism for the cycloaddition reactions of carbonyl compounds to these nucleophilic carbenoid intermediates.

Acknowledgements

This work has been supported by the Ministerio de Economía y Competitividad of the Spanish Government, project CTQ2013-45646-P, by FONDECYT through Project 1140341, by the Millennium Nucleus of Chemical Processes and Catalysis (CPC), grant number NC120082 and by DI-UNAB-793-15/R. M. R.-G. thanks the Ministerio de Economía y Competitividad for a pre-doctoral contract co-financed by the European Social Fund (BES-2014-068258).

References

1 (a) A. Domling, *Chem. Rev.,* 2006, **106**, 17; (b) F. Millich, *Chem. Rev*., 1972, **2**, 101; (c) A. Dömling and I. Ugi, *Angew. Chem., Int. Ed*., 2000, **39**, 3168; (d) A. V. Gulevich, A. G. Zhdanko, R. V. A. Orru and V. G. Nenajdenko, *Chem. Rev.,* 2010, **110**, 5235; (e) S. Sadjadi and M. M. Heravi, *Tetrahedron*, 2011, **67**, 2707; (f) F. De Moliner, L. Banfi, R. Riva and A. Basso, *Comb. Chem. High Throughput Screening*, 2011, **14**, 782; (g) H. R. Sadabad, A. Bazguir, M. Eskandari and R. Ghahremanzadeh, *Monatsh. Chem*, 2014, **145**, 1851; (h) P. Song, L. Zhao, S. Ji, *Chin. J. Chem.* 2014, **32**, 381; (i) T.-H. Zhu, S.-Y. Wang, Y.-Q. Tao, T. Q. Wei and S. J. Ji, *Org. Lett.* 2014, **16**, 12603; (j) Z.-Y. Gu, T.-H. Zhu, J.-J. Cao, X.P. Xu, S.Y. Wang and S.J. Ji, *ACS Catal.* 2014, **4**, 49.

2 (a) V. Nair, A. U. Vinoda, N. Abhilasha, R. S. Menona, V. Santhia, R. L. Varmaa, S. Vijia, S. Mathewa and R. Srinivasb, *Tetrahedron*, 2003, **59**, 10279; (b) V. Nair and A. U. Vinoda, *Chem. Commun.,* 2000, 1019; (c) R. Ghadari, F. Hajishaabanha, M. Mahyari, A. Shaabani and H. R. Khavasi, *Tetrahedron Lett*., 2012, **53**, 4018; (d) A. A. Esmaeili and M. Darbanian, *Tetrahedron*, 2003, **59**, 5545; (e) A. Shaabani, A. H. Rezayan, S. Ghasemi and A. A. Sarvary, *Tetrahedron Lett*., 2009, **50**, 1456.

3 V. Nair and A. U. Vinoda, *Chem. Commun.,* 2000, 1019.

4 (a) A. A. Esmaeili and M. Darbanian, *Tetrahedron*, 2003, **59**, 5545; (b) R. Ghadari, F. Hajishaabanha, M. Mahyari, A. Shaabani and H. R. Khavasi, *Tetrahedron Lett.*, 2012, **53**, 4018.

5 A. Shaabani, A. H. Rezayan, S. Ghasemi and A. A. Sarvary, *Tetrahedron Lett.*, 2009, **50**, 1456.

6 I. Yavari and H. Djahaniani, *Tetrahedron Lett.*, 2005, **46**, 7491.

7 L.-L. Zhao, S.-Y. Wang, X.-P. Xu and S.-J. Ji, *Chem. Commun.*, 2013, **49**, 2569.

8 (a) F. M. Dean, *In Advances in Heterocyclic Chemistry*; Katritzky, A. R., Ed.; Academic: New York, 1982; Vol. 30, pp 167; (b) A. P. Dunlop and F. N. Peters, *The*

Furans; Reinhold: New York, 1953; (c) E. J. Corey and X. M. Cheng, *The Logic of Chemical Synthesis*; Wiley: New York, 1989; (d) R.Benassi, *In Comprehensive Heterocyclic Chemistry II*; A. R. Katritzky, C. W. Rees and E. F. V. Scriven, Eds.; Pergamon: Oxford, 1996; Vol. 2, pp 259; (e) S. Onitsuka and H. Nishino, *Tetrahedron* 2003, **59**, 755; (f) T. Yao, X. Zhang and R. C. Larock, *J. Am. Chem. Soc.* 2004, **126**, 11164; (g) M. Fan, L. Guo, X. Liu, W. Liu and Y. Liang, *Synthesis* 2005, 391; (h) C. K. Jung, J. C. Wang and M. J. Krische, *J. Am. Chem. Soc.* 2004, **126**, 4118; (i) C. Y. Lo, H. Guo, J. J. Lian, F. M. Shen and R. S. Liu, *J. Org. Chem.* 2002, **67**, 3930.

9 W. P. Pei, J. Pei, S. H. Li and X. L. Ye, *Synthesis* 2000, 2069.

10 (a) P. Geerlings, F. De Proft, W.Langenaeker, *Chem. Rev.* 2003, **103**, 1793; (b) D. H. Ess, G. O. Jones, , K. N. Houk *Advanced Synthesis & Catalysis* 2006, **348**, 2337.

11 A. D. Becke and K. E. Edgecombe, *J. Chem. Phys.*, 1990, **92**, 5397

12 X. Krokidis, S. Noury and B. Silvi, *J. Phys. Chem. A*, 1997, **101**, 7277.

13 (a) C. Lee, W. Yang and R. G. Parr, *Phys. Rev. B* 1988, **37**, 785–789; (b) A. D. Becke, *J. Chem. Phys.*, 1993, **98**, 5648.

14 (a) C. E. Check and T. M. Gilbert, *J. Org. Chem.*, 2005, **70**, 9828; (b) G. O. Jones, V. A. Guner and K. N. Houk, *J. Phys. Chem.*, *A* 2006, **110**, 1216; (c) G. A. Griffith, I. H. Hillier, A. C. Moralee, J. M. Percy, R. Roig and M. K. Vicent, *J. Am. Chem. Soc.*, 2006, **128**, 13130; (d) M. Ríos-Gutiérrez, P. Pérez, L. R. Domingo. *RSC Adv.*, 2015, **5**, 58464.

15 Y. Zhao and D. G. Truhlar, *J. Phys. Chem. A*, 2004, **108**, 6908.

16 W. J. Hehre, L. Radom, P. v. R. Schleyer and J. A. Pople, *Ab initio Molecular Orbital Theory*; Wiley: New York, 1986.

17 (a) H. B. Schlegel, *J. Comput. Chem.*, 1982, **2**, 214; (b) H. B. Schlegel, *In Modern Electronic Structure Theory* (Ed.: Yarkony, D. R.); World Scientific Publishing: Singapore, 1994.

18 K. Fukui, *J. Phys. Chem.*, 1970, **74**, 4161.

19 (a) C. González and H. B. Schlegel, *J. Phys. Chem.*, 1990, **94**, 5523; (b) C. González and H. B. Schlegel, *J. Chem. Phys.*, 1991, **95**, 5853.

20 (a) J. Tomasi and M. Persico, *Chem. Rev.*, 1994, **94**, 2027; (b) B. Y. Simkin, I. Sheikhet, *Quantum Chemical and Statistical Theory of Solutions-A Computational Approach* Ellis Horwod: London, 1995.

21 (a) E. Cances, B. Mennucci and J. Tomasi, *J. Chem. Phys.*, 1997, **107**, 3032; (b) M. Cossi, V. Barone, R. Cammi and J. Tomasi, *Chem. Phys. Lett.*, 1996, **255**, 327; (c) V. Barone, M. Cossi and J. Tomasi, *J. Comput. Chem.*, 1998, **19**, 404.

22 (a) A. E. Reed, R. B. Weinstock and F. Weinhold, *J. Chem. Phys.*, 1985, **83**, 735; (b) A. E. Reed, L. A. Curtiss and F. Weinhold, *Chem. Rev.*, 1988, **88**, 899.

23 (a) R. G. Parr and W. Yang, Annu. *Rev. Phys. Chem*., 1995, **46**, 701; (b) H. Chermette, *J. Comput. Chem.,* 1999, **20**, 129; (c) F. De Proft and P. Geerlings, *Chem. Rev*., 2001, **101**, 1451; (d) P. W. Ayers, J. S. M. Anderson and L. J. Bartolotti, *Int. J. Quantum Chem*., 2005, **101**, 520; (e) J. L. Gázquez, *J. Mex. Chem. Soc*., 2008, **52**, 3; (f) R. F. Nalewajski, J. Korchowiec and A. Michalak, in *Density Functional Theory IV, Topics in Current Chemistry*, R. Nalewajski, Ed.,Springer, Berlin, Heidelberg, 1996, vol. 183, p. 25; (g) P. Geerlings, S. Fias, Z. Boisdenghien and F. De Proft, *Chem Soc. Rev*, 2014, **43**, 4989.

24 R. G. Parr, L. von Szentpaly and S. Liu, *J. Am. Chem. Soc.*, 1999, **121**, 1922.

25 (a) R. G. Parr and R. G. Pearson, *J. Am. Chem. Soc.*, 1983, **105**, 7512; (b) R. G. Parr and W. Yang, *Density Functional Theory of Atoms and Molecules*; Oxford University Press: New York, 1989.

26 (a) L. R. Domingo, E. Chamorro and P. Pérez, *J. Org. Chem.*, 2008, **73**, 4615; (b) L. R. Domingo and P. Pérez, *Org. Biomol. Chem.*, 2011, **9**, 7168.

27 W. Kohn and L. J. Sham, *Phys. Rev.*, 1965, **140**, 1133.

28 L. R. Domingo, P. Pérez and J. A. Sáez, *RSC Adv.,* 2013, **3**, 1486.

29 (a) S. Berski, J. Andrés, B. Silvi and L. R. Domingo, *J. Phys. Chem. A*, 2003, **107**, 6014; (b) V. Polo, J. Andrés, S. Berski, L. R. Domingo and B. Silvi, *J. Phys. Chem. A*, 2008, **112**, 7128; (c) J. Andrés, P. González-Navarrete and V. S. Safont, *Int. J. Quant. Chem.*, 2014, **114**, 1239; (d) J. Andrés, S. Berski, L. R. Domingo, V. Polo and B. Silvi, *Curr. Org. Chem.*, 2011, **15**, 3566; (e) J. Andrés, L. Gracia, P. González-Navarrete and V. S. Safont, *Comp. Theor. Chem.,* 2015, **1053**, 17.

30 (a) R. Thom, *Structural Stability and Morphogenesis: An Outline of a General Theory of Models*, Inc.:Reading, MA, 1976; (b) A. E. R. Woodcock and T. Poston, *A Geometrical Study of Elementary Catastrophes*, Spinger-Verlag, Berlin, 1974; (c) R. Gilmore, *Catastrophe Theory for Scientists and Engineers*, Dover: New York, 1981.

31 (a) X. Krokidis, V. Goncalves, A. Savin and B. Silvi, *J. Phys. Chem. A*, 1998, **102**, 5065. (b) X. Krokidis, N. W. Moriarty, W. A. Lester and M. Frenklach, *Chem. Phys. Lett.,* 1999, **314**, 534. (c) I. Fourre, B. Silvi, P. Chaquin and A. Sevin, *J. Comput. Chem.*, 1999, **20**, 897. (d) D. B. Chesnut and L. J. Bartolotti, *Chem. Phys.*, 2000, **257**, 175. (e) F. Fuster, A. Sevin and B. Silvi, *J. Phys. Chem. A*, 2000, **104**, 852. (f) E. Chamorro, J. C. Santos, B. Gomez, R. Contreras and P. Fuentealba, *J. Phys. Chem. A*,

2002, **106**, 11533. (g) P. Chaquin and A. Scemama, *Chem, Phys. Lett.*, 2004, **394**, 244. (h) V. Polo, J. Andrés, R. Castillo, S. Berski and B. Silvi, *Chem. Eur. J.*, 2004, **10**, 5165. (i) V. Polo and J. Andrés, *J. Comput. Chem.*, 2005, **26**, 1427. (j) J. C. Santos, J. Andrés, A. Aizman, P. Fuentealba and V. Polo, *J. Phys. Chem. A*, 2005, **109**, 3687. (k) S. Berski, J. Andrés, B. Silvi and L. R. Domingo, *J. Phys. Chem. A*, 2006, **110**, 13939. (l) V. Polo and J. Andrés, *J. Chem. Theory Comput.*, 2007, **3**, 816. (m) V. Polo, P. Gonzalez-Navarrete, B. Silvi and J. Andrés, *Theor. Chem. Acc.*, 2008, **120**, 341. (n) J. P. Salinas-Olvera, R. M. Gomez and F. Cortes-Guzman, *J. Phys. Chem. A*, 2008, **112**, 2906. (o) I. M. Ndassa, B. Silvi and F. Volatron, *J. Phys. Chem. A*, 2010, **114**, 12900. (p) N. Gillet, R. Chaudret, J. Contreras-Garcia, W. T. Yang, B. Silvi and J. P. Piquemal, *J. Chem. Theory Comput.*, 2012, **8**, 3993.

32 (a) A. Savin, A. D. Becke, J. Flad, R. Nesper, H. Preuss and H. G. Vonschnering, *Angew. Chem. Int. Ed.*, 1991, **30**, 409; (b) B. Silvi and A. Savin, *Nature*, 1994, **371**, 683; (c) A. Savin, B. Silvi and F. Colonna, *Can. J. Chem.*, 1996, **74**, 1088; (d) A. Savin, R. Nesper, S. Wengert and T. F. Fassler, *Angew. Chem. Int. Ed. Engl.*, 1997, **36**, 1808.

33 S. Noury, X. Krokidis, F. Fuster and B. Silvi, *Comput. Chem.*, 1999, **23**, 597.

34 (a) E. R. Johnson, S. Keinan, P. Mori-Sanchez, J. Contreras-Garcia, J. Cohen, A. W. Yang, *J. Am. Chem. Soc.* 2010, **132**, 6498; (b) J. R. Lane, J. Contreras-Garcia, J.-P. Piquemal, B. J.Miller, H. G. Kjaergaard, *J. Chem. Theory. Comput.* 2013, **9**, 3263; (c) J. Contreras-Garcia, E. R. Johnson, S. Keinan, R. Chaudret, J.-P. Piquemal, D. N. Beratan, W. Yang, *J. Chem. Theory. Comput.* 2011, **7**, 625.

35 M. J. Frisch, *et al.*, Gaussian 09, Revision A.02, Gaussian Inc, Wallingford CT, 2009.

36 L. R. Domingo, J. A. Saéz, R. J. Zaragozá, M. Arnó *J. Org. Chem.* 2008, **73**, 8791.

37 L. R. Domingo, *RSC Adv.* 2014, **4**, 32415.

38 L. R. Domingo, M. J. Aurell, P. Pérez, R. Contreras *Tetrahedron* 2002, **58**, 4417

39 P. Jaramillo, L. R. Domingo, E. Chamorro, P. Pérez, *J. Mol. Struct. (Theochem)* 2008, **865**, 68

40 A. Savin, *J. Chem. Sci.*, 2005, **117**, 473.

41 B. Silvi, *J. Mol. Struct.*, 2002, **614**, 3.